IC/91/101
INTERNAL REPORT
(Limited Distribution)

International Atomic Energy Agency
and
United Nations Educational Scientific and Cultural Organization
INTERNATIONAL CENTRE FOR THEORETICAL PHYSICS

HEAVY FRAGMENT RADIOACTIVITY

I. Silisteanu *
International Centre for Theoretical Physics, Trieste, Italy.

ABSTRACT

The effect of collective mode excitation in heavy fragment radioactivity (HFR) is explored and discussed in the light of current experimental data. It is found that the coupling and resonance effects in fragment interaction and also the proper angular momentum effects may lead to an important enhancing of the emission process. New useful procedures are proposed for the study of nuclear decay properties. The relations between different decay processes are investigated in detail. We are also trying to understand and explain in a unified way the reaction mechanisms in decay phenomena.

MIRAMARE – TRIESTE
June 1991

* Permanent address: Institute of Atomic Physics, P.O. Box MG–6, R-76900 Bucharest, Romania.

INTRODUCTION

The renewed interest in heavy fragment radioactivity (HFR) processes sprang up because some experimental data could not be understood within the framework of the solutions proposed earlier. These data include the "fine structure", similar to the alpha decay, and the evidence of the important role of excited states in HFR.

In spite of remarkable progress in untangling and understanding of these new phenomena [1)–10)], some interesting and incomprehensible questions still remain. The most intricating question concerns the significant interplay between the reaction mechanism and the nuclear structure. This question will be investigated in detail in the present paper. For this purpose we would like to extend the lifetime calculations in the spirit of references [7),8)] to all HFR cases so far observed. In our investigations we try to search for answers to the following urgent questions: What are the possibilities for enhancing HFR and how much is the probability of induced HFR (similar to the induced fission)?

1. An outline of the theory

We shall adopt for a description of HFR processes the multichannel approach [8)] which joins together the advantages of the microscopic decay theory and resonance theory of nuclear reactions with the optical model for the emitted fragment. If we consider the decay of the metastable state k of a nucleus into the set c of two body channels, the total width is given by

$$\Gamma_k = 2\pi \sum_c \left| \frac{< u_c^o(r) | I_c^k(r) >}{< u_c^k(r) | I_c^k(r)} \right|^2 \qquad (1)$$

where u_c^{ok} are solutions of systems of differential equations

$$\left[\frac{h^2 d^2}{2 M dr^2} - V_c(r) + \varepsilon_c \right] u_c^{o(k)} - \sum_c V_{cc'}(r)\, u_{c'}^{o(k)}(r) = \left\{ \begin{matrix} 0 \\ I_c^k(r) \end{matrix} \right\} \qquad \begin{matrix} (2) \\ (3) \end{matrix}$$

where:

$M = A_1 \cdot A_2/(A_1 + A_2)$ is the reduced mass of the systems; V_c and $V_{cc'}$ are the diagonal and coupling parts of the interaction potential;

I_c^k is the cluster formation amplitude (CFA);

$\varepsilon_c = E - E_1 - E_2$ is the released energy.

The boundary conditions for the homogeneous system (2) are those imposed for the scattering states. The systems (2,3) are solved numerically in the adiabatic approximation.

Thus, the decay width naturally results from the evolution of formation and penetration probabilities. The usual approach to these probabilities includes the average effects on single particle degrees of freedom in order to obtain CFA and the collective degree of freedom (relative distance between the fragments) for obtaining the interaction potential and finally the decay width.

We construct CFA in the simple shell model approximation [7] and also in the resonance approximation when the metastable state is identified with the lowest resonance state of the compound system at a given decay energy ε_c. The first approximation corresponds to the fragments having the internal degrees of freedom associated to nucleons, while in the second these degrees of freedom are suppressed.

We shall use for the fragment interaction the nuclear potential in conjunction with the Coulomb one. The input parameters used are those which reproduce the measured fusion touching cross sections or reaction cross section data [11)-13)] at energies near the Coulomb barrier. Because the released energies ε_c in HFR are somewhat different from experimental energies we shall modify only the depth of the nuclear potential in order to recover a resonance state in the potential at a given energy. In other words the decaying state is identified with the lowest resonance state of the compound system. In this case the CFA is given by resonance wave function [7]. This, in fact, is just the asymptotic Coulomb CFA. The parameters used for some HFR cases are given in Refs.11–13. It should be mentioned that the potentials resulting from the optical analysis of the fusion and scattering experiments are expected to be very relevant for the calculations of HFR rates.

2. Results

The lifetimes calculated with the prescriptions of Sections 2 and 3 for some HFR cases suggested by Price [14] are presented in Table 1. Column 3 gives the results of the single channel analysis [7] (one decaying state-one open channel) "without" the coupling induced by nuclear deformation. The results of the multichannel analysis (one decaying state – many open channels) which includes the coupling induced by nuclear deformation are given in column 4.

Comparing the results of columns 4 and 5 one may observe that the corrections arising esssentially from low multipole distorsions of the potential at the scission configuration are quite important. The magnitude of these corrections clearly depends on the magnitude of fragment deformations, the maximal corrections corresponding to the large values of nuclear deformations. As a rule, these corrections produce a lifetime decrease by 1–2 orders of magnitude.

Note that the results of Table 1, column 4, together with those of Ref.8 (Table 1, column 5), represent a complete lifetime multichannel account which covers all current experimental information on HCR.

The present study also confirms the conclusion of Ref.8 – the HFR may be enhanced if the collective degrees of freedom of the fragments are excited.

3. Comparison of cluster models

Table 2 shows in columns 3–5 the emission rates predicted by the simple cluster models [5)-7)] and in column 6 the experimental rates. The common approach to these models includes the average over single particle degrees of freedom in order to obtain a reasonable estimation

for CFA. In spite of rather different approaches for CFA the agreement of the calculated and experimental rates is remarkable.

The CFA results in the semi–empirical approach [6] from fitting the α–formation date, while in our approach CFA is obtained numerically by averaging over the shell model α–formation amplitudes. In the former case the preformation factors used $S_\alpha = 5.3 \times 10^{-3}$ (even parent), $S_\alpha = 3.2 \times 10^{-3}$ (odd parent).

In our case S_α depends on the structure of the single particle configuration used, finally the CFA being a Gaussian function of the relative distance between fragments. For completeness, we also calculate the so–called experimental spectroscopic factor (ESF).

$$S_c = \Gamma^{exp}/\Gamma^{res} \tag{4}$$

where Γ^{exp} is the experimental cluster decay width and Γ^{res} is the resonance decay width arising only from the proper transmission probability (the correct asymptotic CPA being the resonance wave function of the compound system (see Ref.7).

The ratio (4) may be looked at as a global measure of the contribution of all structure effects to the decay width. The calculated ESF are presented in Table 3 (column 4). Here one may observe:

i) The ESF is practically constant for a given type of HFR.

ii) The ESF decreases with the increasing mass of the emitted fragment.

iii) Even–odd effects in HFR are clearly transposed in ESF.

If we introdcue the following parametrization in complete analogy with the one for α–decay

$$S_c = S_\alpha^{n_\alpha + (A_2 - 4n_\alpha)/4} \tag{5}$$

where n_α is the number of α–particles, then from S_c values (Table 3) one may deduce the mean value of the alpha spectroscopic factor S_α. For all the observed HFR S_α varies between $0.17\ 10^{-3}$ (^{34}Si from ^{241}Am) and $6.8\ 10^{-3}$ (^{24}Ne from ^{236}U). These values are in good agreement with those calculated by Blendowske and Wallisser [6].

4. Short comment of HFR data and theoretical models

A detailed comparison of the data with the results predicted by theoretical models is made in Ref.10. In addition, we want to point out that:

1. The Geiger–Muttal law, $\log T = AQ^{-1/2} + B$, is strictly verified for measured HFR cases, as well as in α–decay (see Fig.1).

2. The dependence of $\log T_c$ on the fissionability parameter $X = Z_1 Z_2 / A^{1/3}$ is very different from the one observed for experimental fission lifetimes (see Fig.2). Note that the released energy Q increases with the barrier high (Fig.3) as well as the mean kinetic energy in fission.

3. With the increasing mass of the emitted cluster lifetimes of HFR vary between α and fission lifetimes (Fig.4). From a theoretical point of view all the decay rates (alpha, cluster and fission) may be understood as a barrier penetration phenomenon slowed down by the formation probability factor.

4. The inclusion of degrees of freedom such as deformation [2] I, paring [15], collective rotation [8] leads to important corrections to the decay rates that may improve the accord to the data. Usually, in Refs.1 and 4, the exact boundary conditions at small and large distances are not imposed in the dynamical description of the process. Therefore, the resonant aspects of the phenomenon and asymptotic normalizations of formation and penetration probabilities are also neglected. Furthermore, the excited states [16] are not explicitly treated.

In our method, these difficulties in the dynamical treatment of the decay are eliminated from the beginning. But, the shell model approach for CFA usually needs [7] tedious calculations and finally, a very long computing time.

The major part of lifetime calculation in both the macroscopic and microscopic treatments is contained in penetrability integral associated with the post–scission barrier, determined by the interaction energy of final fragments. In the regime between last contact and infinite separation. This major part can be estimated accurately provided realistic nuclear radii and nucleus α–nucleus potentials are used.

The most difficult part of lifetime calculation concerns the region between the ground state of the parent and the last contact (scission) configuration.

In the macroscopic treatment this region is treated as a simple extension of the barrier (one dimensional) penetrability problem by using empirically information on the barrier at both ends of the regime. It should be stressed here that the information on the left end (inner) of the barrier remains uncertain and quite conventional, while that the information on the right end are more complete being supported by scattering data.

In the microscopic treatment this part of calculation is estimated in general case by considering the preformations as part of the process of barrier penetration itself. Thus, the CFA controlates the penetrability of this regime.

CONCLUSIONS

The excitation of the collective degrees of freedom connected with deviations from the sphericity of the fragments leads to significant corrections in the emission rates of HFR. Furthermore, the excitation of rotational and low–vibrational states appears as an important mechanism for enhancing the HFR. The experimental investigation of the problem is already available with the current detection technique.

The study of the relevant degrees of freedom in spontaneous nuclear decays reveals [17] new interesting aspects and allows a deep understanding of these phenomenon. It is hoped that this beginning of an investigation will prove useful to the analysis and the understanding of the "fine structure" [16] recently discovered in the ^{14}C emission from ^{223}Ra.

Acknowledgments

The author would like to thank Professor Abdus Salam, the International Atomic Energy and UNESCO for hospitality at the International Centre for Theoretical Physics, Trieste.

REFERENCES

1) D.N. Poenaru, M. Ivascu, A. Sandulescu and W. Greiner, Phys. Rev. **C32**, 572 (1984).

2) Y.I. Shi and W.J. Swiatecki, Nucl. Phys. **A464**, 205 (1987).

3) G.A. Pik–Pichak, Sov. J. Nucl. Phys. **44**, 923 (1986).

4) G. Shanmugan and B. Kamalaharam, Phys. Rev. **C38**, 1377 (1988).

5) B. Buck and A.C. Marchant, J. Phys. G. Nucl. Part. Phys. **15**, 615 (1989).

6) R. Blendowske and H. Walliser, Phys. Rev. Lett. **61**, 1930 (1988).

7) M. Ivascu and I. Silisteanu, Nucl. Phys. **A485**, 93 (1988).

8) I. Silisteanu and M. Ivascu, J. Phys. G. Nucl. Part. Phys. **15**, 1405 (1989).

9) M. Iriondo, D. Jerrestam and R.J. Liotta, Nucl. Phys. **A454**, 252 (1986).

10) P. Price Buford, Nucl. Phys. **A502**, 41C and references therein.

11) B.B. Beck, R.R. Bets, J.E. Gindler. B.D. Wilkins, S. Saini, M.B. Tsang, C.K. Gelbke, W.G. Lynch, M.A. Mc Mahan and P.A. Baisden, Phys. Rev. **C32**, 195 (1985).

12) J.J. Kolota, K.E. Rehm, D.G. Kovar, G.S.F. Stephans, H.I. Rosner Kezoe and P. Waitecle, Phys. Rev. **20**, 125 (1984).

13) R.P. Cristiansen and A. Winther, Phys. Lett. **B65**, 19 (1977).

14) P. Price Buford, private communciation.

15) F. Baranco, R.A. Brooglia, G.F. Bertch, Phys. Rev. Lett. **60**, 507 (1988).

16) L. Brillard, A.G. El Ayi, E. Hourani, M. Hussonnois, J.F. Le Du, L.H. Rosver and L. Stab, C.R. Acad. Sci. Paris **39**, ser.2, 1105 (1989).

17) M. Ivascu and I. Silisteanu, Sov. J. Part. and Nuclei, Vol.21, **6**, 1405 (1990).

TABLE CAPTIONS

Table 1 Halftime calculations for HFR cases [14] within two different procedures [7),8)] without and with nuclear deformation. The resonance parameters of the potential are used in both types of calculations (see text).

Table 2 Nuclei with measured partial halflives for HFR and the results predicted by the cluster models.

Table 3 The experimental and resonance decay widths for HFR and their corresponding spectroscopic factors (see text).

Table 1

Decay	Q MeV	log $T^{calc}(s)$ Ref.7	log $T^{calc}(s)$ Ref.8	log $T^{exp}(s)$ Ref.10
$^{221}Fr \rightarrow {}^{14}C + {}^{107}Tl$	31.285	20.18	18.74	>15.77
$^{221}Ra \rightarrow {}^{14}C + {}^{207}Pb$	32.400	19.17	17.62	>14.35
$^{225}Ac \rightarrow {}^{14}C + {}^{211}Si$	30.470	23.51	22.13	>18.34
$^{231}Pa \rightarrow {}^{23}F + {}^{208}Pb$	51.831	25.63	24.42	>24.61
$^{230}Th \rightarrow {}^{24}Ne + {}^{206}Hg$	57.766	26.42	25.16	24.64 ± 0.07
$^{232}Th \rightarrow {}^{26}Ne + {}^{206}Hg$	56.581	23.89	26.71	>27.94
$^{233}U \rightarrow {}^{25}Ne + {}^{208}Pb$	60.832	26.15	24.24	24.83 ± 0.15
$^{234}U \rightarrow {}^{24}Ne + {}^{210}Pb$	58.830	27.99	25.78	25.25 ± 0.05
$^{234}U \rightarrow {}^{26}Ne + {}^{208}Pb$	60.083	28.84	26.07	25.25 ± 0.05
$^{237}Np \rightarrow {}^{30}Ng + {}^{207}Tl$	75.706	28.56	27.69	>27.27
$^{238}Pu \rightarrow {}^{28}Mg + {}^{210}Pb$	75.915	25.87	24.93	25.70 ± 0.25
$^{238}Pu \rightarrow {}^{30}Mg + {}^{208}Pb$	76.710	28.47	26.15	25.70 ± 0.15
$^{238}Pu \rightarrow {}^{32}Si + {}^{206}Hg$	91.208	27.74	26.33	25.30 ± 0.16

Table 2

Decay	E MeV	log $T(s)$ 5	6	7	10	log $T^{exp}(s)$ 10
$^{221}Fr \rightarrow {}^{14}C$	29.28	14.00	15.5	20.18	16.2	>15.77
$^{221}Ra \rightarrow {}^{14}C$	30.34	12.40	14.2	19.17	14.1	>14.35
$^{222}Ra \rightarrow {}^{14}C$	30.87	11.2	11.8	10.5	11.2	11.02 ± 0.06
$^{223}Ra \rightarrow {}^{14}C$	29.85	15.3	15.1	14.9	15.0	15.2 ± 0.05
$^{224}Ra \rightarrow {}^{14}C$	28.63	16.1	16.2	15.3	16.0	15.9 ± 0.12
$^{225}Ac \rightarrow {}^{14}C$	28.57	18.8	18.6	23.51	18.7	>18.34
$^{226}Ra \rightarrow {}^{14}C$	26.46	21.2	21.1	21.7	21.0	21.33 ± 0.2
$^{231}Pa \rightarrow {}^{23}F$	46.68	-	-	25.63	26.0	>24.61
$^{230}Th \rightarrow {}^{24}Ne$	51.75	24.4	24.8	26.42	24.8	24.64 ± 0.07
$^{232}Th \rightarrow {}^{26}Ne$	49.70	28.7	27.9	28.89	29.1	>27.94
$^{231}Pa \rightarrow {}^{24}Ne$	54.14	21.6	23.4	23.9	23.7	23.38 ± 0.08
$^{232}U \rightarrow {}^{24}Ne$	55.86	20.2	20.8	19.8	20.7	21.06 ± 0.1
$^{233}U \rightarrow {}^{24}Ne$	54.27	23.7	25.4	24.4	24.4	24.83 ± 0.15
$^{233}U \rightarrow {}^{25}Ne$	54.32	-	-	26.25	25.7	24.83 ± 0.15
$^{234}U \rightarrow {}^{24}Ne$	52.81	25.5	25.6	27.99	25.8	25.25 ± 0.05
$^{234}U \rightarrow {}^{26}Ne$	52.87	25.9	26.4	28.84	26.2	25.25 ± 0.05
$^{234}U \rightarrow {}^{28}Mg$	65.26	25.7	25.4	25.7	25.4	25.75 ± 0.06
$^{237}Np \rightarrow {}^{30}Mg$	65.52	27.3	29.9	26.47	27.5	>27.27
$^{238}Pu \rightarrow {}^{30}Mg$	67.00	25.6	25.8	28.47	25.9	25.7 ± 0.15
$^{238}Pu \rightarrow {}^{28}Mg$	67.32	25.7	26.9	25.87	25.5	25.7 ± 0.25
$^{238}Pu \rightarrow {}^{32}Si$	78.95	26.0	25.7	27.74	25.7	25.3 ± 0.16
$^{241}Am \rightarrow {}^{34}Si$	80.60	25.3	28.8	28.8	26.5	>25.3

Table 3

	Decay	Γ^{exp} (MeV)	Γ^{rec} (MeV)	S_c
1	^{221}Fr ^{14}C	0.775 (-37)	0.913 (-26)	0.848 (-11)
2	^{221}Ra ^{14}C	0.204 (-35)	0.671 (-24)	0.304 (-11)
3	^{222}Ra ^{14}C	0.440 (-32)	0.202 (-21)	0.217 (-10)
4	^{223}Ra ^{14}C	0.303 (-36)	0.228 (-26)	0.132 (- 9)
5	^{224}Ra ^{14}C	0.629 (-37)	0.858 (-27)	0.773 (-10)
6	^{225}Ac ^{14}C	0.209 (-39)	0.769 (-28)	0.271 (-11)
7	^{226}Ra ^{14}C	0.285 (-42)	0.105 (-31)	0.276 (-10)
8	^{231}Pa ^{23}F	0.112 (-45)	0.713 (-31)	0.157 (-14)
9	^{230}Th ^{24}Ne	0.104 (-45)	0.257 (-31)	0.404 (-14)
10	^{232}Th ^{26}Ne	0.523 (-49)	0.670 (-35)	0.780 (-14)
11	^{231}Pa ^{24}Ne	0.176 (-44)	0.781 (-29)	0.225 (-15)
12	^{232}U ^{24}Ne	0.460 (-42)	0.901 (-27)	0.510 (-15)
13	^{235}U ^{24}Ne	0.699 (-46)	0.649 (-30)	0.107 (-15)
14	^{233}U ^{25}Ne	0.691 (-46)	0.504 (-29)	0.137 (-16)
15	^{234}U ^{24}Ne	0.257 (-46)	0.280 (-33)	0.917 (-13)
16	^{234}U ^{26}Ne	0.257 (-46)	0.139 (-31)	0.184 (-15)
17	^{234}U ^{28}Mg	0.606 (-47)	0.517 (-31)	0.117 (-15)
18	^{237}Np ^{30}Mg	0.245 (-48)	0.994 (-32)	0.246 (-16)
19	^{238}Pu ^{30}Mg	0.910 (-47)	0.397 (-31)	0.229 (-15)
20	^{238}Pu ^{28}Mg	0.910 (-47)	0.522 (-31)	0.174 (-15)
21	^{238}Pu ^{32}Si	0.292 (-46)	0.766 (-31)	0.381 (-15)
22	^{241}Am ^{34}Si	0.113 (-46)	0.407 (-30)	0.277 (-16)

FIGURE CAPTIONS

Fig.1 Geiger–Muttal plott for nuclei with measured halflives for HFR and alpha–decay (right lower part).

Fig.2 Experimental halflives for fission and HFR plotted as a function of fissionability parameter Z^2/A.

Fig.3 HFR emission energy represented as a function of the Coulomb barrier height.

Fig.4 Experimental halflives for alpha–decay, HFR and fission plotted as a function of the proton number Z. The alpha and fission halflives correspond to the most living isotopes.

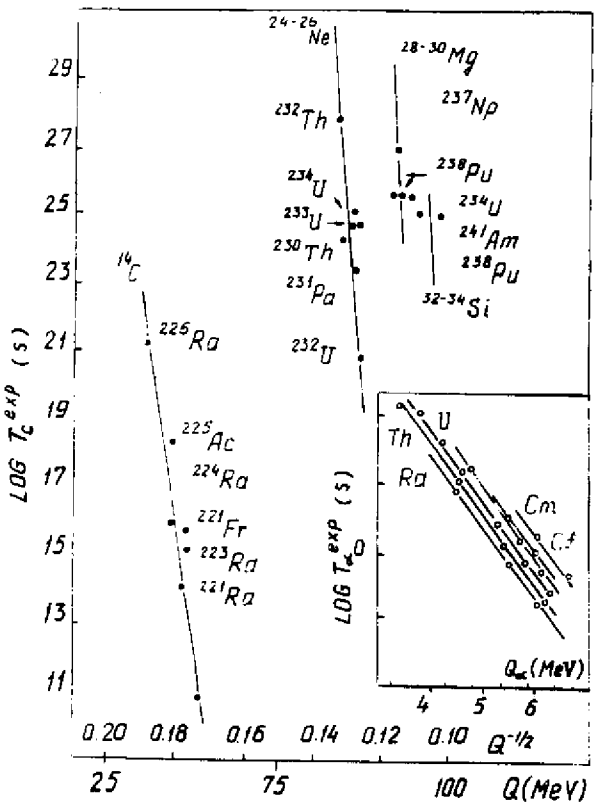

Fig.1

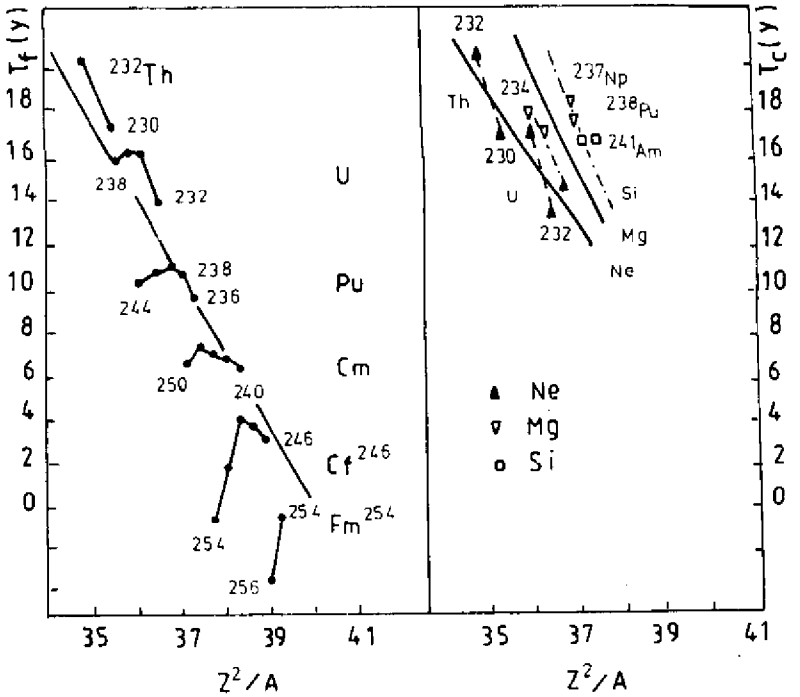

Fig.2

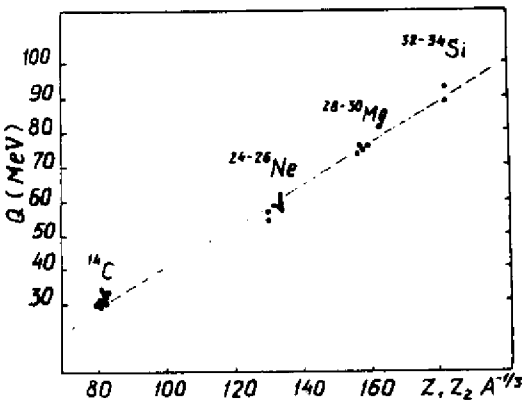

Fig.3

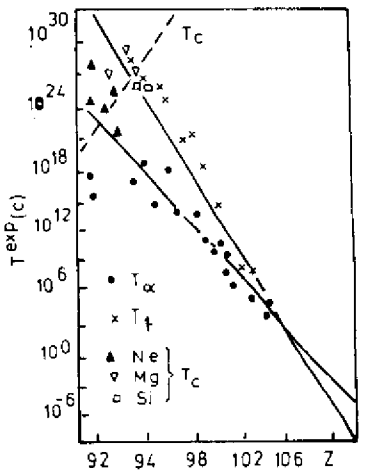

Fig.4